ZAMM · Z. Angew. Math. Mech. **83**, No. 2, 93 – 104 (2003) / **DOI** 10.1002/zamm.200310009

Modelling nonlinear dynamics of shape-memory-alloys with approximate models of coupled thermoelasticity

R. V. N. Melnik[1,*] **and A. J. Roberts**[2]

[1] University of Southern Denmark, Mads Clausen Institute, 6400 Sønderborg, Denmark
[2] Department of Mathematics and Computing, University of Southern Queensland, QLD 4350, Australia

Received 7 February 2001, revised 13 March 2002, accepted 4 April 2002
Published online 27 January 2003

Key words nonlinear thermoelasticity, shape-memory alloys, differential-algebraic solver, center manifold technique
MSC (2000) 35Q72, 65M20, 74F05

We present a general methodology for constructing approximate models describing shape memory alloys dynamics. We base our discussion on a general three-dimensional model and the Falk-Konopka representation for the free energy function. By considering a one-dimensional counterpart of that model, we show that with little computational efforts we can reproduce successfully phase transition phenomena with our numerical scheme. The same scheme is applied in our code for the general case. Then, we describe a systematic approach to modelling SMA materials, and demonstrate that approach in deriving a centre-manifold-based low-dimensional model from the general three-dimensional model, preserving all main features of the dynamics. Computer algebra technique allows us to derive such models efficiently and with arbitrary degree of accuracy.

1 Introduction

Phase transitions are universal phenomena [22], and their adequate description with tools of mathematical modelling represents a challenging task in applied mathematics and mechanics. In this paper we concentrate on mathematical models for the description of a specific type of phase transitions, solid-solid phase transitions, observed in materials with memory, in particular in shape memory alloys. It is well known that some materials such as metals, polymers, ceramics are able to change their crystallographic structure depending on the stress and the temperature. Moreover, some of them can be "smart" enough to restore their original shapes under the action of such physical fields as thermal, mechanical, magnetic, or even hydrostatic after being deformed. Our interest here is the thermomechanical phase transitions. This class of phase transitions has attracted a considerable attention of researchers during recent years (e.g., see [6, 8, 33, 23, 12, 13, 11, 27, 20] and references therein). It is well understood that in describing the dynamics of shape memory alloys it is important to account for the coupling of the three main physical quantities of continuum mechanics (stresses, deformation gradients, and displacements) to the thermal field. In some cases, additional effects should be taken into account, e.g. the rate of thermal disturbances and the relaxation time of thermal fluxes. The importance of these effects, in particular in modelling short transient states in low temperature regimes, is known from the dynamic hyperbolic thermoelasticity where mathematical procedures and computational techniques have a longer history compared to those for SMA applications [19, 34]. In this paper we provide the reader with a model that takes into account finite speeds of thermal disturbances. Models based on the classical Fourier laws follow from our model as special cases in the limit of zero relaxation time for heat fluxes. We allow for the dependency of stresses not only on the deformation gradient and temperature but also on the rates of their changes. Such considerations put us closer to real situations where the time-dependent coupling between temperature and stresses have to include the velocity of the deformation gradient and the speed of thermal propagation. Another distinctive feature of the present consideration is that we use the nonlocal theory of continuum mechanics which considers constitutive variables defined at a point as a function of their values over the whole spatial domain of interest rather than as a function at that point only [2]. The importance of nonlocal models in modelling phase transitions in solids has been recently re-emphasised in [4].

A number of computational results describing the dynamics of phase transitions based on different mathematical models have been already reported in the literature (see, e.g. [23, 14, 1, 20] and references therein). Since most reported results have been obtained with one-dimensional models and little is know about the applicability of models for SMA materials in the general 3D case, in this paper we aim at developing a general strategy for deriving such low-dimens ional models that are able to capture all essential feature of the SMA dynamics, starting from the general 3D consideration.

The paper is organized as follows.

* Corresponding author, e-mail: rmelnik@mci.sdu.dk

 0044-2267/03/8302-0093 $ 17.50+.50/0

- In Section 2 we discuss a general 3D model describing the dynamics of SMA materials giving a specific example based on the Falk-Konopka representation of the free energy function.
- Section 3 is devoted to a one-dimensional counterpart of the above model. Constitutive equations are discussed in detail for this case, and an efficient numerical procedure based on a reduction of the PDE-based model to a system of differential-algebraic equations is exemplified with representative computational examples.
- The same procedure has been already applied to our low-dimensional models derived rigorously from the general 3D considerations in Section 4. This section provides the reader with the basis of a systematic approach for deriving a hierarchy of mathematical models. The approach is based on the centre manifold technique, and is explained in detail from both theoretical and numerical view points. A specific example of the model obtained by applying this technique is given.
- Concluding remarks and fu ture directions are addressed in Section 5.

2 Nonlocal models for solid-solid phase transitions and constitutive relationships

Our consideration rests on a coupled system of three fundamental laws, that is mass, momentum, and energy balances for a system occupying volume $\mathcal{V}$ and having spatial reference configuration Ω at time t_0 in the Lagrangian (material) system of coordinates $(\mathbf{x}, t)$ with $\mathbf{x} = (x_1, x_2, x_3)$. Let $\mathbf{u} = (u_1, u_2, u_3)$ be the displacement vector, e be the internal energy of the system per unit mass, $\mathbf{v} = \partial\mathbf{u}/\partial t$ be the velocity, $\rho(\mathbf{x}, t)$ be the density at $(\mathbf{x}, t)$, and $\mathbf{q}$ be the heat flux. Then, our model can be written as

$$\begin{aligned} &\rho\frac{\partial^2\mathbf{u}}{\partial t^2} = \nabla_{\mathbf{x}}\cdot\mathbf{s} + \mathbf{F},\\ &\rho\frac{\partial e}{\partial t} - \mathbf{s}^T : (\nabla\mathbf{v}) + \nabla\cdot\mathbf{q} = g\,. \end{aligned} \tag{2.1}$$

Nonlocal effects are easily incorporated into the model. In particular, we can write that $\mathbf{F} = \rho(\mathbf{f} + \hat{\mathbf{f}}) - \hat{\rho}\mathbf{v}$ (e.g., [21]), $\mathbf{a}^T : \mathbf{b} = \sum_{i,j=1}^{3} a_{ij}b_{ij}$, $g = \rho(h + \hat{h}) - \rho\hat{\mathbf{f}}\cdot\mathbf{v} - \hat{\rho}\left(e - \mathbf{v}^2/2\right)$, $\mathbf{v}^2 = \mathbf{v}\cdot\mathbf{v}$, where h is the heat source density, $\hat{h}$ is the nonlocal energy residual (see [2] for conditions on localised residuals), $\mathbf{f}$ is a given body force per unit mass, $\hat{\rho}$ and $\hat{\mathbf{f}}$ are nonlocal mass and force residuals, respectively, and $\mathbf{s}$ is the stress tensor.

In the most general consideration $\rho(\mathbf{x}, t)$ need not be the same at $t = t_0 + \Delta t$ and at t_0. In other words, the balance of mass in the form $\rho(\mathbf{x}, t)\det(\mathbf{I} + \boldsymbol{\epsilon}(\mathbf{x}, t)) = \rho_0(\mathbf{x}, t_0)$, with $\rho_0(\mathbf{x}, t_0) > 0$ being the density of the matter in the reference configuration Ω at time t_0, can also be incorporated. We require that $\det(\mathbf{I} + \boldsymbol{\epsilon}(\mathbf{x}, t))$ where the strain tensor $\boldsymbol{\epsilon}(\mathbf{x}, t))$ is introduced by $\boldsymbol{\epsilon} = \mathrm{sym}\,[\partial\mathbf{u}(\mathbf{x}, t)/\partial\mathbf{x}]$. Note that a nonlocal theory that we develop in a small strain framework might not account for the fact that a single crystal SMA can exist in multiple stress-free configurations. However, the procedure proposed in Section 4 can also be applied in the finite-strain theory framework where one can include the inelastic strain effects. To make the discussion transparent to the reader, in what follows we concentrate on the Cauchy strain tensor only.

The right-hand sides of eqs. (2.1) incorporate into the model nonlocal and dissipative effects of thermomechanical waves. As we shall see in the next section, under appropriate constitutive relations it is also possible to allow for a relaxation time for acceleration of the motion in response to applied gradients such as the deformation gradient and the temperature gradient. It is not our purpose here to go into discussion about the choice of the free energy function (see [10, 22] for these issues); we just postulate that it can be defined in the Helmholtz form

$$\Psi(\boldsymbol{\epsilon}, \theta) \equiv e - \theta\eta = \psi^0(\theta) + \sum_{n=1}^{\infty}\psi^n(\boldsymbol{\epsilon}, \theta)\,, \tag{2.2}$$

with the entropy density η defined by $\eta = -\partial\Psi/\partial\theta$, the temperature of the system θ such that $\theta > 0$, and $\inf_{(\mathbf{x},t)}\theta = 0$, and independent material parameters of the n-th order for $n = 1, 2, ...$ determined through strain invariants, $\mathcal{I}_j^n$, as follows:

$$\psi^n = \sum_{j=1}^{j^n}\psi_j^n\mathcal{I}_j^n \quad \text{and} \quad \psi^0(\theta) = \psi_0(\theta)\,, \tag{2.3}$$

where j^n is the number of all invariant directions associated with a representation of the 48th order cubic symmetry group of the parent phase (see details in [7]). Other representations (e.g., those where strain-gradient terms are involved) are possible, and can be incorporated into the model we shall discuss in Section 4. For example, the Fremond-type models (e.g., [8]) use different expressions for free energy functions for different phases, which have the Landau-Devonshire-Ginzburg forms and contain the term $\gamma/2\nabla\mathrm{tr}(\boldsymbol{\epsilon})$ with $\gamma > 0$. This term can smooth spatial phase separations (see further comments in [21]). The free energy function employed here is based on the expansion up to sixth order in strain components which proved to be an adequate approximation for a range of SMA materials in both 1D and 3D cases (e.g., [6, 7]). Note, however, that in the later

case one cannot use the shear strain as the order parameter as we often do for the 1D case. Finally, it should be also noted that it is a simple algebraic procedure to incorporate higher order terms in a systematic methodology to SMA modelling proposed in Section 4.

In the 3D case 32 material parameters that are required for our approximation is already a formidable experimental task and the results of measurements related to these parameters are sketchy in the literature. That is why we concentrate here on a specific class of SMA alloys, namely the copper-based alloys for which the representation (2.3) requires experimental data on 10 parameters only. We concentrate on this case in detail in Section 4. Implementing other possible free energy functions which might be more appropriate for other classes of SMA materials follow the pattern explained here. Our particular form is

$$\Psi = \psi^0(\theta) + \sum_{j=1}^{3} \psi_j^2 \mathcal{I}_j^2 + \sum_{j=1}^{5} \psi_j^4 \mathcal{I}_j^4 + \sum_{j=1}^{2} \psi_j^6 \mathcal{I}_j^6, \tag{2.4}$$

where the strain invariants $\mathcal{I}_i^n$ of second, forth, and sixth orders of the 48th order cubic symmetry group of the parent phase are given in the form proposed in [7]

$$\begin{aligned}
&\mathcal{I}_1^2 = \frac{1}{9}(\mathrm{tr}(\epsilon_{ij}))^2,\ \ \mathcal{I}_2^2 = \frac{1}{12}(2\epsilon_{33} - \epsilon_{11} - \epsilon_{22})^2 + \frac{1}{4}(\epsilon_{11} - \epsilon_{22})^2,\ \ \mathcal{I}_3^2 = \epsilon_{23}^2 + \epsilon_{13}^2 + \epsilon_{12}^2,\\
&\mathcal{I}_1^4 = (\mathcal{I}_2^2)^2,\ \ \mathcal{I}_2^4 = \epsilon_{23}^4 + \epsilon_{13}^4 + \epsilon_{12}^4,\ \ \mathcal{I}_1^6 = (\mathcal{I}_2^2)^3\ ,\ \ \mathcal{I}_3^4 = (\mathcal{I}_3^2)^2,\ \ \mathcal{I}_4^4 = \mathcal{I}_2^2\mathcal{I}_3^2,\\
&\mathcal{I}_5^4 = \epsilon_{23}^2 \left[\frac{1}{6}(2\epsilon_{33} - \epsilon_{11} - \epsilon_{22}) - \frac{1}{2}(\epsilon_{11} - \epsilon_{22})\right]^2\\
&\qquad + \epsilon_{13}^2 \left[\frac{1}{6}(2\epsilon_{33} - \epsilon_{11} - \epsilon_{22}) + \frac{1}{2}(\epsilon_{11} - \epsilon_{22})\right]^2 + \frac{1}{9}\epsilon_{12}^2(2\epsilon_{33} - \epsilon_{11} - \epsilon_{22})^2,\\
&\mathcal{I}_2^6 = \frac{1}{36}(2\epsilon_{33} - \epsilon_{11} - \epsilon_{22})^2 \left(\frac{1}{36}(2\epsilon_{33} - \epsilon_{11} - \epsilon_{22})^2 - \frac{1}{4}(\epsilon_{11} - \epsilon_{22})^2\right)^2.
\end{aligned} \tag{2.5}$$

Coefficients ψ_j^n should be experimentally fitted and in the general case are temperature dependent, e.g. we take $\psi_3^2 = (1.48 \times 10^6 - 940(\theta - 300))\ \mathrm{g}/(\mathrm{ms}^2\mathrm{cm})$. All coefficients used here have the same forms as those given in [7, 18].

Having defined the free energy function the internal energy function e is given by

$$e = \Psi - \theta \frac{\partial \Psi}{\partial \theta}. \tag{2.6}$$

Finally, we have to specify the constitutive relationships that couple stresses, deformation gradients, temperature, and heat fluxes:

$$\Phi_1(\mathbf{s}, \boldsymbol{\epsilon}) = 0\,, \quad \Phi_2(\mathbf{q}, \theta) = 0\,, \tag{2.7}$$

where it is implicitly assumed that these relations may involve spatial and temporal derivatives of the functions.

If the Cattaneo-Vernotte model is used in the constitutive relation for Φ_2, it is postulated that

$$\mathbf{q} + \tau_0 \frac{\partial \mathbf{q}}{\partial t} = -k(\theta, \boldsymbol{\epsilon}) \nabla \theta\,, \tag{2.8}$$

with the dimensionless thermal relaxation time τ_0, and the thermal conductivity of the material $k(\theta, \boldsymbol{\epsilon})$. Then we can rewrite our energy balance equation in the form

$$\rho \frac{\partial e}{\partial t} + \rho\tau_0 \frac{\partial^2 e}{\partial t^2} - \mathbf{s}^T : (\nabla \mathbf{v}) - \tau_0 \frac{\partial}{\partial t}[\mathbf{s}^T : (\nabla \mathbf{v})] - \nabla \cdot (k \nabla \theta) = G\,, \tag{2.9}$$

where $G = g + \tau_0 \partial g / \partial t$. Such a choice is made in order to account for the finite speeds of thermal wave propagation and thermally induced stress wave propagation coupled to the deformation gradient [34].

We assume that the shear stress in eq. (2.1) is determined by its three components, the quasi-conservative component, $\mathbf{s}^q$, the stress component due to mechanical dissipation, $\mathbf{s}^m$, and the stress component due to thermal dissipations, $\mathbf{s}^t$ (the latter is assumed to be negligible at this stage),

$$\mathbf{s} = \mathbf{s}^q + \mathbf{s}^m + \mathbf{s}^t \quad \text{with} \quad \mathbf{s}^q = \rho \frac{\partial \Psi}{\partial \boldsymbol{\epsilon}}, \quad \mathbf{s}^m = \rho\mu \frac{\partial \boldsymbol{\epsilon}}{\partial t}, \quad \mathbf{s}^t = \mathbf{0}. \tag{2.10}$$

In the general case the heat flux is determined as the solution of eq. (2.8). An approximation to this solution is provided by the generalised form of the Fourier law $\mathbf{q} = -k\nabla\theta - \alpha \partial k \nabla \theta / \partial t$, $\alpha \geq 0$, which we will use with $\alpha = 0$ when it turns into the classical Fourier law. Finally, we have to supplement system (2.1) by appropriate initial, and boundary conditions as explained in [21]. In what follow, we exemplify our numerical procedures applied to models described in this section with representative computational results, and describe a systematic approach to modelling of shape memory alloy dynamics.

3 Approximating shape-memory-alloy dynamics and setting the scene for computational experiments

In this section we apply the developed models to the description of shape memory alloy effects in a rod. It is well-known that for many types of shape memory materials the dependency of stresses on the deformation gradient upon loading and unloading is significantly different. Applying a large load at a low temperature, we may get a residual deformation gradient, which typically vanishes upon heating. The restoring of the original shape, that is the shape memory effect, is demonstrated with representative numerical examples that follow. All results are obtained by using an effective numerical procedure based on a reduction of the original system of PDEs to a system of differential-algebraic equations.

A key to the understanding of solid-solid phase transitions is kept by the coupling of mechanical and thermal fields. This coupling is realised in model (2.1) by the choice of the free energy function. Before proceeding to our general procedure for deriving a hierarchy of approximate models, we sketch briefly main points in the one-dimensional modelling of shape memory alloys (e.g., [12, 33, 23, 14, 21] and references therein). A one-dimensional analogue of the general form of the free energy function presented in Section 2 is known as the Landau-Devonshire model (see also comments on the Landau-Devonshire-Ginzburg models in [21]). The rationale behind this and other similar models, which goes back to Landau's works on phase transitions and Falk's generalisation of those results to solid-solid phase transitions, is to take care not only for mechanical and thermal energy contributions, but also for their intrinsic nonlinear coupling by choosing the free energy function in the form $\Psi(\theta,\epsilon)=\psi_0(\theta)+\psi_1(\theta)\psi_2(\epsilon)+\psi_3(\epsilon)$. While, as seen from notation, $\psi_0(\theta)$ gives "purely" thermal contributions to the energy, $\psi_3(\epsilon)$ gives "purely" mechanical contributions, the term $\psi_1(\theta)\psi_2(\epsilon)$ is aimed at the modelling of coupling contributions. In the context of the Landau-Devonshire model these functions are defined as $\psi_0(\theta)=\alpha_0-\alpha_1\theta\ln\theta$, $\psi_1(\theta)=\frac{1}{2}\alpha_2\theta$, $\psi_2(\epsilon)=\epsilon^2$, $\psi_3(\epsilon)=-\frac{1}{2}\alpha_2\theta_1\epsilon^2-\frac{1}{4}\alpha_4\epsilon^4+\frac{1}{6}\alpha_6\epsilon^6$ with some positive constants α_i, $i=1,2,4,6$, and θ_1.

Compared to the general 3D case, the definition of the stress-strain relationship is straightforward in the one-dimensional case [6, 12, 23, 33]. Even in the relatively difficult case of the dependency of stress on the rate of deformation gradient and temperature [21], i.e. where

$$s=\rho\left[p(\theta,\epsilon)+\lambda\left(\frac{\partial\theta}{\partial t}\,,\quad\frac{\partial\epsilon}{\partial t}\right)\right]\quad\text{with}\quad\lambda\left(\frac{\partial\theta}{\partial t},\frac{\partial\epsilon}{\partial t}\right)=\tilde{\mu}(\theta)\frac{\partial\epsilon}{\partial t}+\tilde{\nu}(\epsilon)\frac{\partial\theta}{\partial t}\,,$$

it is easy to deduce that $p(\theta,\epsilon)=\partial\Psi/\partial\epsilon=\alpha_2\epsilon(\theta-\theta_1)-\alpha_4\epsilon^3+\alpha_6\epsilon^5$, because in the one-dimensional case macroscopic strain can be chosen as an order parameter in the model, providing a link to microscopic deformations at the lattice structure level. Now, without going into any further detail we formulate our one-dimensional model

$$\begin{aligned}
&C_v\left[\frac{\partial\theta}{\partial t}+\tau_0\frac{\partial^2\theta}{\partial t^2}\right]-k_1\left[\theta\frac{\partial u}{\partial x}\frac{\partial^2 u}{\partial t\partial x}+\tau_0\frac{\partial}{\partial t}\left(\theta\frac{\partial u}{\partial x}\frac{\partial^2 u}{\partial t\partial x}\right)\right]\\
&-\mu\left[\left(\frac{\partial^2 u}{\partial t\partial x}\right)^2+\tau_0\frac{\partial}{\partial t}\left(\frac{\partial^2 u}{\partial t\partial x}\right)^2\right]-\nu\left[\frac{\partial\theta}{\partial t}\frac{\partial^2 u}{\partial t\partial x}+\tau_0\frac{\partial}{\partial t}\left(\frac{\partial\theta}{\partial t}\frac{\partial^2 u}{\partial t\partial x}\right)\right]-\frac{\partial}{\partial x}\left(k\frac{\partial\theta}{\partial x}\right)=G\,,\\
&\rho\frac{\partial^2 u}{\partial t^2}-\frac{\partial}{\partial x}\left[k_1\frac{\partial u}{\partial x}(\theta-\theta_1)-k_2\left(\frac{\partial u}{\partial x}\right)^3+k_3\left(\frac{\partial u}{\partial x}\right)^5\right]-\mu\frac{\partial^3 u}{\partial x^2\partial t}-\nu\frac{\partial^2\theta}{\partial x\partial t}=F\,,
\end{aligned}\tag{3.1}$$

where $C_v=\rho\alpha_1$, $k_1=\rho\alpha_2$, $k_2=\rho\alpha_4$, $k_3=\rho\alpha_6$, $\mu=\rho\tilde{\mu}$, $\nu=\rho\tilde{\nu}$. Further details and discussion on initial and boundary conditions can be found in [21]. A detailed description of an efficient numerical procedure based on a reduction of the model to a system of differential-algebraic equations is given in [21]. Two representative results of applications of that procedure to modelling mechanically- and thermally-induced phase transitions are demonstrated by Figs. 1 and 2, respectively. These computational experiments were conducted with no stress dependency on the rate of θ and ϵ for a 1cm copper-based SMA rod (see parameters in [20]). In Fig. 1 mechanically driven transformations are shown. Results are obtained with no thermal forcing $G=0$, and with the time-varying mechanical forcing given by $F=7000\sin^3(\pi t/2)$ $\mathrm{g}/(\mathrm{cm}^2\mathrm{ms}^2)$. Under initial conditions $u^0=0$ and $\theta^0=255\mathrm{K}$ these results are in a good agreement with the previously reported experiments [14]. A more challenging situation lies with thermally-driven phase transformations (as well as a combination of thermal and mechanical forcings, see further details on that in [20]). In Fig. 2 we start from a $2M^+ + 2M^-$ martensite configuration by choosing the initial temperature at $\theta^0=200\mathrm{K}$, and the initial displacements $u^0(x)=ax+b$ with $a=-0.11809, b=0$ for $x\in[0,1/6]$; $a=0.11809, b=0.11809/3$ for $x\in[1/6,1/2]$; $a=-0.11809, b=2/3*0.11809$ for $x\in[1/2,5/6]$; and $a=0.11809, b=-0.11809$ for $x\in[5/6,1]$. This is a different computer experimental setup compared to the already reported results, e.g. in [23], where the standard martensitic twins were used for the initial conditions. The mechanical forcing in our experiment was unchanged in time at $F=500\mathrm{g}/(\mathrm{ms}^2\mathrm{cm}^2)$ and the thermal forcing was given by $G=375\pi\sin^3(t\pi/6)\mathrm{g}/(\mathrm{ms}^3\mathrm{cm})$. Observe that after a transformation to the austenite phase due to the temperature increase, the stable attractor upon the return to the low-temperature is not the original configuration, but rather a twin martensite. This is confirmed by the next austenite-to-martensite transformation, as seen in Fig. 2. Further computational experiments demonstrating effectiveness of the developed numerical procedure based on the reduction of the original model to a system of differential-algebraic equations can be found in [20]. This procedure is also efficient for centre-manifold reductions of the general 3D models. Now, we are in a position to describe a general algorithm for obtaining such reduced, approximate models.

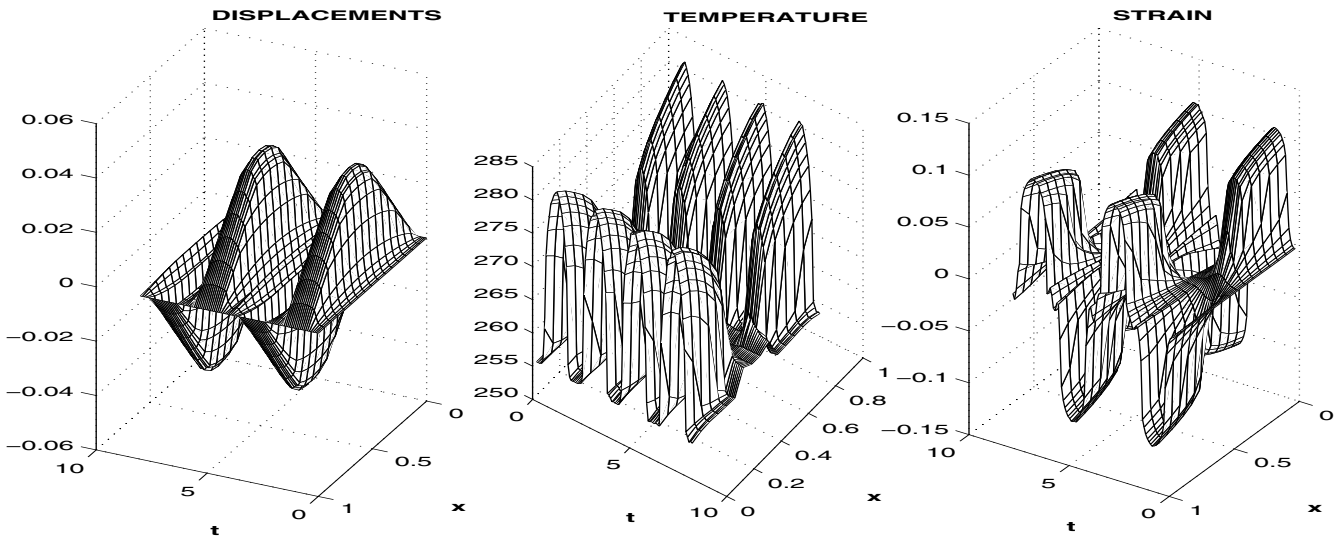

Fig. 1 Mechanically induced phase transitions

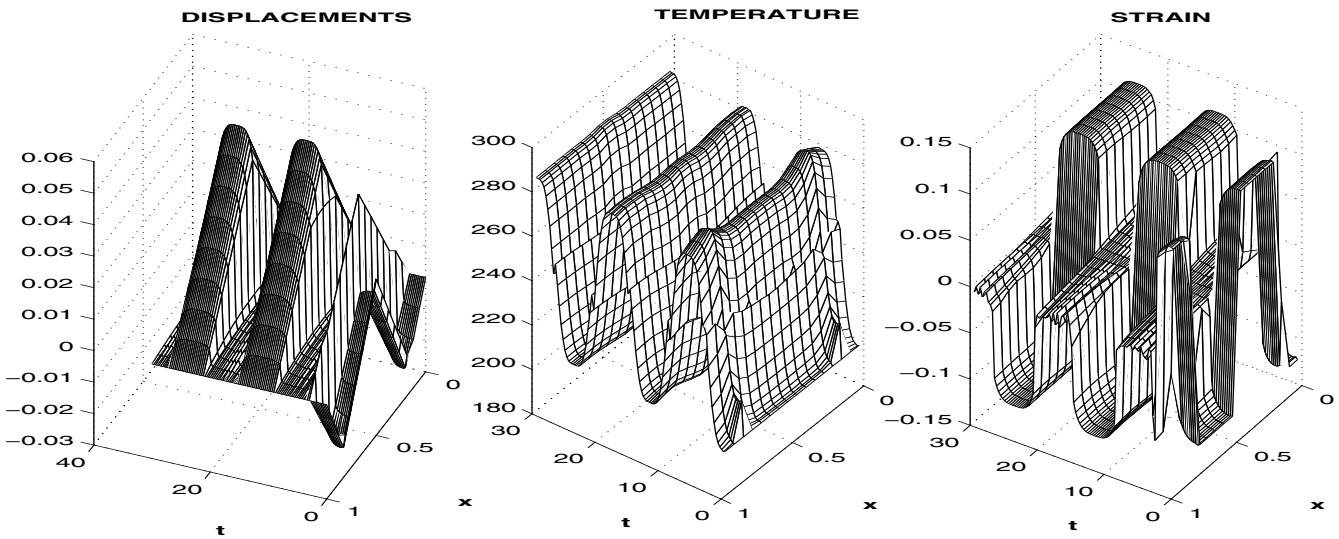

Fig. 2 Thermally induced phase transformations

4 General 3D models for SMA dynamics with centre manifold approximations

As we have shown in the previous section, the behaviour of SMA materials is fairly complicated even in the one-dimensional case to rend the researchers some "easy" solutions in the adequate description of the dynamics of these materials. Complicated nonlinearities in models for the SMA description leave little chances for success in investigating the SMA dynamics by means of analytical tools, and the development of new efficient numerical techniques is required. Another important point we would like to make in this context is that although theoretical investigations of phase transitions and hysteresis effects achieved some maturity [3, 15], little is known so far on how one can simplify *systematically* higher dimensional models appearing in the literature for the description of these materials.

Therefore, here we aim at developing a systematic approach to SMA modelling, starting from our general 3D model described in Section 2. Our "battle horse" in this task will be the centre manifold technique. Hence, it is appropriate to recall basic ideas on which the application of this technique rests before proceeding to our specific low-dimensional model for the description of shape memory alloy dynamics.

4.1 Slow and fast motions in infinite-dimensional dynamic systems

The idea to split the motion of dynamic systems into components, e.g. "fast" (or high frequency) and "slow" (or low frequency), has been been employed in mathematical and engineering literature for quite some time. For example, this idea is central to the treatment of singular perturbed type systems since Tichonov's works on the subject. By now, the subject has been developed

substantially by the efforts of many researchers in the contexts of differential equations, control theory, and applications (e.g., [17] and references therein).

In the context of this paper we recall that many dissipative evolutionary systems can be cast mathematically in the following form (e.g., [31]):

$$\frac{d\mathbf{u}}{dt} + \mathcal{A}\mathbf{u} = -\mathbf{F}(\mathbf{u}), \tag{4.1}$$

where $\mathbf{u}$ is the evolving variable (vector function), $\mathcal{A}$ is a linear operator, and $\mathbf{F}$ is a nonlinear vector function. Such models have been studied by employing different techniques. One such a technique is based on the notion of inertial manifold applicable to both finite and infinite dimensional systems (e.g., [9, 31] and references therein). If we assume that the motion of the system takes place in a Hilbert space H and, under appropriate conditions, associate the system with a semigroup $S(t) : \mathbf{u}_0 \to \mathbf{u}(t), \quad t \geq 0, \quad \mathbf{u}(0) = \mathbf{u}_0$, then an inertial manifold of this system is introduced as a finite dimensional Lipschitz manifold $\mathcal{M}$ such that $\mathcal{M}$ attracts exponentially all the orbits of (4.1) and $S(t)\mathcal{M} \subset \mathcal{M}\ \forall t \geq 0$, i.e., $\mathcal{M}$ is positively invariant for the semigroup S. There are several difficulties in computing such inertial manifolds. To explain the roots of those difficulties one should recall that the analysis of inertial manifolds rests on *the exponential decay towards the global attractor* [30]. This typically requires a quite restrictive condition, known as the spectral gap condition. In particular, assuming that $\mathcal{A}$ is self-adjoint with compact $\mathcal{A}^{-1}$ and a set of eigenvalues λ_j and eigenfunctions $\boldsymbol{\omega}_j$ such that $\mathcal{A}\boldsymbol{\omega}_j = \lambda_j\boldsymbol{\omega}_j$, $\lambda_{j+1} \geq \lambda_j$ (e.g., [31]), this condition can be formulated as

$$\lambda_{n+1} - \lambda_n > 2C_1(\lambda_n^{\alpha-\beta} - \lambda_{n+1}^{\alpha-\beta}), \tag{4.2}$$

where $\alpha, \beta \in \mathbb{R}$ such that map $\mathbf{f} \equiv -\mathbf{F} : D(\mathcal{A}^\alpha) \to D(\mathcal{A}^\beta)$ is globally bounded (see details, e.g., in [31]). This condition leads to *asymptotically complete inertial manifolds* $\mathcal{M}_a$,

$$|\mathcal{A}^\alpha[\mathbf{u}(t) - \mathbf{v}(t)]| \leq C(|\mathbf{A}^\alpha\mathbf{u}_0|)\exp(-kt), \quad \mathbf{v}(t) \in \mathcal{M}, \quad k > 0, \tag{4.3}$$

meaning that for any $\mathbf{u}_0$ there is a trajectory $\mathbf{v}(t)$ on $\mathcal{M}_a$ to which the $\mathbf{u}(t)$-trajectory through $\mathbf{u}_0$ is asymptotic. This idea leads to a hint on how to compute *approximate inertial manifolds* (AIM), which might not be inertial in the above-mentioned sense. Many constructed procedures in this field rely on the following representation:

$$\mathcal{M}_a = \Gamma[\boldsymbol{\varphi}] \equiv \{\mathbf{p} + \boldsymbol{\varphi}(\mathbf{p}) : \mathbf{p} \in P_nH\}, \tag{4.4}$$

where P_n is the finite-dimensional projection operator with the generalised Fourier basis $\{\boldsymbol{\omega}_i\}$ such that $P_n\mathbf{u} = \sum_{i=1}^n(\mathbf{u}, \boldsymbol{\omega}_i)\boldsymbol{\omega}_i$, and $\boldsymbol{\varphi}$ is from a space typically defined by making use of the spectral gap condition. Then, different numerical procedures can be exploited in order to approximate $\boldsymbol{\varphi}$, and obtain an AIM following some exponential tracking rules. One of the most popular approaches in this case is to use the nonlinear Galerkin method. Calculating inertial manifolds is also a popular technique in the context of postprocessing the Galerkin (both standard and nonlinear) procedures [16, 9]. The reason for this popularity is based on the fact that after spatially discretising an infinite-dimensional PDE-based model and obtaining a system of differential-algebraic equations, it is quite natural to try to split the resulting system into "slow" and "fast" components, and then try to "slave" the dynamics of the quick subsystem to the slow one during numerical integration by using some rules. While in calculating approximate inertial manifolds the development of such "slaving rules" stems from the desire to inherit the asymptotic completeness property of the original inertial manifold by the developed approximations, we base our consideration upon the local exponential decay (e.g., [30]) rather than on the global asymptotic "slaving" rules. The centre manifold technique is at the origin of the development of many efficient computational schemes for the solution of (4.1) as well as for the postprocessed Galerkin methodologies [16, 28]. The application of this technique does not require to invoke a very restrictive spectral gap condition and to find the global eigenfunctions of the linear dynamics [30]. For such complex PDE-based systems as those dealt with in this paper the centre manifold technique provides a general framework for the computational analysis with a high degree of flexibility to modify the model, to include new additional effects as new experimental data become available, and to construct new approximate models to the existing ones with arbitrary accuracy.

4.2 Centre manifold theory and the main steps of the computational algorithm

The centre manifold technique has been successful in solving many important problems in science and engineering (e.g., [28, 29, 30] and references therein). The invariant sets are at the heart of studying dynamics [26], and when it comes to infinite-dimensional systems a key to the understanding of their dynamics is kept by our ability to reduce the system dimensionality and to restrict our attention to an invariant subspace, known as the centre manifold, which contains all of the essential dynamics of the system. It is known that the qualitative change in the behaviour of a nonlinear system of arbitrary dimension can be established by analysing the linearised Jacobian's eigenvalues associated with the subset of eigenvalues having zero real parts. This means that the centre manifold technique can effectively deal with non-hyperbolic invariant sets (which cannot be persistent in general) by allowing us *to construct* a reduced system describing the dynamics on a manifold that is associated with non-hyperbolic (critical) eigenvalues, i.e. linearised eigenvalues having zero real parts. The idea to find such a centre manifold

containing the invariant set with the smallest possible dimension originates from a seminal paper [25] where the classical centre manifold technique was introduced for a special case of (4.1) in the form of the ODE such as $\mathbf{u}' = \mathbf{f}(\mathbf{u})$. It was shown that under appropriate regularity assumptions there exists a centre manifold in a neighbourhood of a non-hyperbolic equilibrium $\mathbf{u}_0$ which is tangent to the generalised eigenspace of $\mathbf{J}\mathbf{f}(\mathbf{u}_0)$ with Jacobian $\mathbf{J}$ associated with those non-hyperbolic (critical) eigenvalues [5]. This concept has been spread to partial differential equations, in particular in the form of inertial manifolds as we discussed in the previous subsection. The general theory of approximation dynamics has been extended further to cover more and more complicated dynamic behaviours (see [26] and references therein). A quite general result on the existence of centre manifold has been recently derived in [5]. The result holds true for a very large class of invariant (admissible) sets that includes smooth manifolds with corners, unions of compact manifolds, and Lipschitz manifolds, and the reader interested in theoretical aspects of centre manifold should consult [28, 5] for further detail. Here we recall that the application of the centre manifold technique rests on the three main theorems, known as the existence, relevance, and approximation theorems. We say that the centre manifold $\mathcal{M}_c$ is a manifold to which all trajectories in *the neighbourhood* of a fixed point are attracted exponentially quickly. Then, under appropriate conditions (e.g., [32, 28] and references therein) we can claim that

- the original dynamics has a centre manifold with low-dimensional dynamics in the Pliss sense;
- the dynamics on a finite-dimensional centre manifold models adequately the original dynamics in a sense that starting from a set of initial conditions all solutions of the original dynamics tend to a solution on the centre manifold exponentially quickly;
- if in the construction of a centre manifold we can satisfy the governing equations of the model to some order of accuracy, then the centre manifold is given to the same order of accuracy.

Two remarks should be given in this context.

Remark 4.1. A centre manifold needs not be unique, but the differences between the possible centre manifolds are of the same order as the differences we set out to ignore in establishing the low-dimensional model. Hence, when and if non-uniqueness arises, it is irrelevant to modelling.

Remark 4.2. The centre manifold technique allows us to derive not only governing equations for the model, but also initial and boundary conditions (see [28, 29] and references therein).

The approach has a straightforward geometric interpretation (e.g. [28]). In the context of our model we can say that if the amplitudes of the modes of SMA dynamics are viewed as coordinates in a state space then the dynamic behaviour of the SMA system corresponds to motion along some trajectory. When many of the modes are rapidly decaying, trajectories are quickly attracted to some low-dimensional invariant manifold, which may be parametrised *by the amplitudes of the critical modes*. Since SMA materials have several different equilibrium configurations (austenite and martensite), it is also appropriate to note that our approach does not need to be linked to just the one equilibrium.

Consider now a general parametrised family of models (4.1)

$$\frac{d\mathbf{u}}{dt} = \mathcal{L}\mathbf{u} + \mathbf{f}(\mathbf{u}, \boldsymbol{\varepsilon}), \tag{4.5}$$

where $\boldsymbol{\varepsilon}$ is a vector of parameters, and $\mathcal{L} = -\mathcal{A}$ is a linear operator with discrete spectrum which separates into eigenvalues of zero real-part, i.e. the critical eigenvalues, and eigenvalues with strictly negative real-part, $\mathbf{f}$ is at least quadratic nonlinear function in both $\mathbf{u}$ and $\boldsymbol{\varepsilon}$, as they tend to zero (see [28] for further details and illustrative examples). This parametrised family is quite rich and includes as a special case perturbed systems (4.1) such as (e.g., [31])

$$\frac{d\mathbf{u}}{dt} + \epsilon\mathcal{A}\mathbf{u} = \mathbf{f}(\mathbf{u}) \quad \Longrightarrow \quad \frac{d\mathbf{u}}{dt} + \mathcal{A}\mathbf{u} = \epsilon^{-1}\mathbf{f}(\mathbf{u}), \tag{4.6}$$

where the right part is obtained from the left part by rescaling the time, $\tau = t/\epsilon$ with $\epsilon > 0$, a technique often used in the singular perturbation theory. This idea is often used in the inertial manifold approach with the introduction of a prepared equation associated with a truncated form of (4.1) which is typically obtained by using a *single* parameter such as ϵ in order to scale all others. Our model (4.5) covers a more general situation where the traditional scaling procedure mentioned above might not be appropriate. This is the case when one has to deal with several different interacting fields, e.g. where the interacting mechanical waves, coupled to the thermal field, could travel with different speeds. In such situations, representing all effects at leading order of a single small parameter can result in misleading outputs. What is needed in such situations is a careful balancing of the order of small effects in the model construction rather than at the stage of the application of the model. One of the most appealing features of the centre manifold technique in such application areas as those considered in this paper is that not only it allows us an effective treatment of *many different small effects* by choosing as many orders in the amplitudes and as many different parameters as needed, but also it shows the way to a consistent truncation procedure at the stage when the model is applied (see [28, 29] and references therein).

Certainly, the direct application of power series for such complex infinite dimensional systems as those considered in Section 2 is prohibitive even for the computer due to a quick growth of terms that are required to be accounted for. On the other hand, after the model has been constructed a balancing of the the order of small effects might still be required, and the application of such methodologies as the multiple scale method could again lead to unreasonably heavy computational tasks. To increase the efficiency of computational procedures and to develop a basis for *systematically* reducing the dimension of complex dynamic systems (4.5), while retaining their essential properties, we use a different idea. After ε in (4.5) is chosen to measure the contribution of small effects, the idea is to express our model in terms of asymptotic sums in ε, and then to balance carefully the order of these effects at *the stage of the model construction*. In what follows we concentrate on the situation where the critical eigenvalues of $\mathcal{L}$ are exactly zero of arbitrary multiplicity, taken here as M (see comments and further details on the treatment of the critical eigenvalues with a non-zero imaginary part in [28]). If we denote the "amplitudes" of those eigenvalues by U_i, $i = 1, ..., M$, then by the centre manifold relevance theorem their evolution in time forms an accurate low-dimensional model of the original dynamic system, that is such a low-dimensional model of the original infinite-dimensional system described by our system of PDEs is valid exponentially in time. Therefore, based on the model (4.5) we aim at finding a low-dimensional model

$$\frac{d\mathbf{U}}{dt} = \mathbf{g}(\mathbf{U}), \quad \mathbf{U} \in \mathbb{R}^M \ , \tag{4.7}$$

for the evolution of M "amplitudes" $\mathbf{U}$. These low-dimensional dynamics occur on the exponentially attractive centre manifold which may be described parametrically as

$$\mathbf{u} = \boldsymbol{\nu}(\mathbf{U}), \tag{4.8}$$

where $\boldsymbol{\nu}$ is a vector function to be found. As we shall see, this function can be found approximately with arbitrary degree of accuracy by using computer algebra. Our computational algorithms consists of three main steps [28]:

- We identify the M critical modes by finding the nontrivial solutions of $\mathcal{L}\boldsymbol{\nu} = 0$ denoted further by $\boldsymbol{\nu}_i$, $i = 1, ..., M$, and provide a new approximate model to the original dynamics on a linear approximation to the centre manifold written here in terms of modal amplitudes U_i:

$$\mathbf{u}(t) \approx \sum_{i=1}^{M} \boldsymbol{\nu}_i U_i = \mathcal{N}\mathbf{U} \quad \text{such that} \quad \frac{d\mathbf{U}}{dt} \approx \mathbf{G}\mathbf{U}, \tag{4.9}$$

  where $\mathbf{G}$ may be chosen in Jordan form (in the general case the critical eigenspace is needed, and hence all the generalised eigenvector modes should be determined), and $\boldsymbol{\nu}$ is approximated linearly at this stage of the procedure by using matrix $\mathcal{N} = [\boldsymbol{\nu}_1, ..., \boldsymbol{\nu}_M]$. This first step in projecting the linear and nonlinear parts of the original dynamics onto the slow modes of interest should be modified by nonlinear terms which leads us to the next step of the algorithm.
- In order to obtain the actual nonlinear "shape" of the centre manifold characterising the original nonlinear dynamics, we perform an iterative procedure to modify our linear approximation from the previous step. This procedure is organised in a spirit of Newton's iterations in a sense that it is aimed at iterative modifications of the centre manifold to a specified level of description by finding such a low-dimensional model that satisfies the original model (4.5) with the pre-defined accuracy. More precisely, we use the centre manifold approximation theorem [28] to drive the residuals of the governing equations to the pre-defined accuracy. Let us describe this procedure in some detail [28]
  - Assume that at iteration k we already have the following approximate model:

$$\mathbf{u}(t) \approx \boldsymbol{\nu}^k(\mathbf{U}) \quad \text{such that} \quad \frac{d\mathbf{U}}{dt} \approx \mathbf{G}^k(\mathbf{U}), \tag{4.10}$$

    where $\boldsymbol{\nu}^k$ and G^k denote approximations to $\boldsymbol{\nu}$ and $\mathbf{g}$, respectively, at iteration k. If the residual of the governing eq. (4.5) at this stage is estimated as

$$\frac{d\mathbf{u}}{dt} - \mathcal{L}\mathbf{u} - \mathbf{f}(\mathbf{u}, \boldsymbol{\varepsilon}) = \frac{\partial \boldsymbol{\nu}^k}{\partial \mathbf{U}}\mathbf{g}^k - \mathcal{L}\boldsymbol{\nu}^k - \mathbf{f}(\boldsymbol{\nu}^k, \boldsymbol{\varepsilon}) = \mathcal{O}(\|\mathbf{U}\|^{\beta_1}, \|\boldsymbol{\varepsilon}\|^{\beta_2}), \tag{4.11}$$

    for some orders of error denoted here as β_1 and β_2, we can find corrections $\Delta\boldsymbol{\nu}$ and $\Delta\mathbf{g}$ such that the following model

$$\mathbf{u} \approx \boldsymbol{\nu}^k(\mathbf{U}) + \Delta\boldsymbol{\nu}(\mathbf{U}) \quad \text{such that} \quad \frac{d\mathbf{U}}{dt} \approx \mathbf{g}^k(\mathbf{U}) + \Delta\mathbf{g}(\mathbf{U}) \ , \tag{4.12}$$

    is a *higher order approximation to the original dynamics*.
  - Improving at each iteration the order of error in terms on β_1 and β_2, we improve the accuracy of the model according to the centre manifold approximation theorem [28]. This is achieved by substituting (4.12) into the governing eq. (4.5), and solving a new problem with respect to the correction terms $\Delta\boldsymbol{\nu}$ and $\Delta\mathbf{g}$:

$$\left(\frac{\partial \boldsymbol{\nu}^k}{\partial \mathbf{U}} + \frac{\partial \Delta\boldsymbol{\nu}}{\partial \mathbf{U}}\right)(\mathbf{g}^k + \Delta\mathbf{g}) = \mathcal{L}\boldsymbol{\nu}^k + \mathcal{L}\Delta\boldsymbol{\nu} + \mathbf{f}(\boldsymbol{\nu}^k + \Delta\boldsymbol{\nu}, \boldsymbol{\varepsilon}). \tag{4.13}$$

This problem is solved in an iterative manner with respect to $\Delta\boldsymbol{\nu}$ and $\Delta\mathbf{g}$ which introduce error $\mathcal{O}(\|\mathbf{U}\|^{\beta_1+1} + \|\boldsymbol{\varepsilon}\|^{\beta_2+1})$ into approximation (4.12). Ignoring smaller terms (that is the higher order terms, in particular those of $\mathcal{O}(\|\mathbf{U}\|^{2\beta_1} + \|\boldsymbol{\varepsilon}\|^{2\beta_2})$ order, rearranging the resulting terms, and using the "approximate" chain rule (e.g., that $\partial\boldsymbol{\nu}^k/\partial\mathbf{U}\mathbf{g}^k = \partial\boldsymbol{\nu}/\partial t$ since $\mathbf{g}^k = \partial\mathbf{U}/\partial t$) the main block of the iterative sub-procedure is reduced to the solution of the equation

$$\mathcal{L}\Delta\boldsymbol{\nu} - \mathcal{N}\Delta\mathbf{g} = \mathbf{r} \quad \text{where} \quad \mathbf{r} = \frac{\partial\boldsymbol{\nu}^k}{\partial t} - \mathcal{L}\boldsymbol{\nu}^k - \mathbf{f}(\boldsymbol{\nu}^k, \varepsilon), \tag{4.14}$$

requiring the evaluation of the residual at iteration k (see details in [28]). At each iteration of this sub-procedure we deal with physically meaningful expressions (as an example, see our comments to (4.23) in Section 4.3), while the evaluation of the residual is performed efficiently with a computer algebra package, in our case with Reduce.

- Then, we use (4.12) to update the approximation of the centre manifold, and subsequently to construct a higher order accuracy approximate model to the original dynamics.

Now we are in a position to apply the described algorithm to the construction of low-dimensional models capturing all the essential features of the dynamics of materials with memory in higher dimensions.

4.3 Exemplification for the 3D Falk-Konopka model

We are interested in the construction of an adequate model for the description of thermomechanical behaviour of thin slabs in shape memory alloy materials. Starting from the 3D Falk-Konopka model and using centre manifold techniques we derive systematically an accurate low-dimensional model for the dynamics of the slab. The shape memory alloy is assumed to be of very large extent in the $x = x_1$ direction compared to its thickness of $2b$ in the $y = x_2$ direction ($-b < y < b$). For the sake of convenience we use a new temperature variable $\theta' = \theta - \theta_0$ where here $\theta_0 = 300$. For simplicity of the analysis we assume zero dissipation, $\alpha = \mu = \nu = 0$, and that there is no motion nor dependence in the x_3 direction.

A model for the dynamics of modes which vary slowly along the slab is derived for the unforced dynamics, $\mathbf{F} = \mathbf{0}$, $G = 0$, and when "zero-stress & thermal-insulation" boundary conditions are specified on $y = \pm b$. The derivation of boundary conditions in the "long" direction x requires a quite delicate analysis and these issues will not be address here (for details see [28, 29] and references therein). We only note that "pinned & insulating ends" boundary conditions may be used as a leading approximation. Modelling the long-wavelength, small-wavenumber modes along the slab, we neglect all longitudinal variations and look for eigenvalues of the cross-slab modes. It can be shown that generally there is a zero eigenvalue of multiplicity five and all the rest are pure imaginary (as dissipation has been omitted). Thus there exists a sub-centre manifold based upon these five modes (see [32] for an existence theorem), called a slow manifold as these five modes evolve slowly. Note that being on a sub-centre manifold the models we construct only have a weak assurance of asymptotic completeness, and therefore the spectral gap condition is not required for the construction (see [28, 29] and references therein). The zero eigenvalue of multiplicity five corresponds to longitudinal waves, large-scale bending, and one heat mode. The leading order structure of the critical eigenmodes are constant across the slab. Thus letting an overbar denote the y average, the amplitudes of the critical modes are chosen in the form

$$U_i(x,t) = \overline{u_i}\,, \quad V_i(x,t) = \overline{v_i}\,, \quad \Theta'(x,t) = \overline{\theta'}\,. \tag{4.15}$$

The low-dimensional model given below as an example is written in terms of these parameters. The construction of the low-dimensional model is based upon the ansatz that there exists a low-dimensional invariant manifold upon which the amplitudes evolve slowly:

$$u_i = \mathcal{U}_i(\boldsymbol{U}, \boldsymbol{V}, \Theta')\,, \quad v_i = \mathcal{V}_i(\boldsymbol{U}, \boldsymbol{V}, \Theta')\,, \quad \theta = \mathcal{T}(\boldsymbol{U}, \boldsymbol{V}, \Theta')\,, \tag{4.16}$$

$$\text{where} \qquad \frac{\partial U_i}{\partial t} = V_i\,, \quad \frac{\partial V_i}{\partial t} = g_i(\boldsymbol{U}, \boldsymbol{V}, \Theta')\,, \quad \frac{\partial \Theta'}{\partial t} = g_\theta(\boldsymbol{U}, \boldsymbol{V}, \Theta')\,, \tag{4.17}$$

and g_1, g_2, and g_θ have the same meaning as components of the vector function $\mathbf{g}$ in (4.7). After spatially discretising (2.1), this ansatz is substituted into the resulting differential-algebraic equations of 3D thermoviscoelasticity (see details in [21]), and is solved to some order in the small parameters ∂_x, $E = \|\boldsymbol{U}_x\| + \|\boldsymbol{V}_x\|$, and $\vartheta = \|\Theta'\|$ with the computer algebra package Reduce (see, e.g., [28] and references therein). Thus, here we treat the strains as small, as measured by E, while permitting asymptotically large displacements and velocities. The displacement and temperature fields of the slow manifold, in terms of

the amplitudes and the scaled transverse coordinate $Y = y/b$, are found approximately:

$$u_1 \approx U_1 - Yb\frac{\partial U_2}{\partial x} + 0.15(3\,Y^2-1)b^2\frac{\partial^2 U_1}{\partial x^2}\,, \tag{4.18}$$

$$\begin{aligned} u_2 \approx\ & U_2 - (0.9 - 3.05\times10^{-5}\Theta')Yb\frac{\partial U_1}{\partial x} + 0.15(3\,Y^2-1)b^2\frac{\partial^2 U_2}{\partial x^2} \\ & - 141\,Yb\left(\frac{\partial U_1}{\partial x}\right)^3 + 1.00\times10^{-4}(3Y-Y^3)b^3\left(\frac{\partial V_1}{\partial x}\right)^2\frac{\partial U_1}{\partial x}\,, \end{aligned} \tag{4.19}$$

$$\begin{aligned} \theta \approx\ & 300 + \Theta' - 2.43\text{e}6\,(3Y-Y^3)b^3\left(\frac{\partial V_1}{\partial x}\frac{\partial^2 U_2}{\partial x^2} + \frac{\partial U_1}{\partial x}\frac{\partial^2 V_2}{\partial x^2}\right) \\ & - 25.1(7 - 30\,Y^2 + 15\,Y^4)\left(\frac{\partial V_1}{\partial x}\right)^3\frac{\partial U_1}{\partial x}\,. \end{aligned} \tag{4.20}$$

These expressions have errors $\mathcal{O}\left(E^5 + \partial_x^{5/2} + \vartheta^{5/2}\right)$ where the notation $\mathcal{O}\left(E^p + \partial_x^q + \vartheta^r\right)$ is used to denote terms involving $\partial_x^{\beta_2}E^{\beta_1}\vartheta^{\beta_3}$ such that $\beta_1/p + \beta_2/q + \beta_3/r \geq 1$. Note that the mechanical and thermal field approximations represented by (4.18)–(4.20) have cross-slab structure. In particular, recall [18] that the sideways deformation u_2 (which is a nonlinear function of the longitudinal strains) of the shape memory alloy feed back at higher order to contribute to and complicate the longitudinal and thermal dynamics.

The model for the longitudinal dynamics on this slow manifold is

$$\begin{aligned} \rho\frac{\partial V_1}{\partial t} =\ & c_1\frac{\partial^2 U_1}{\partial x^2} + \gamma_1 b^2\frac{\partial^4 U_1}{\partial x^4} \\ & + \frac{\partial}{\partial x}\left[(c_2\Theta' - c_3\Theta'^2)\frac{\partial U_1}{\partial x} - (c_4 - c_5\Theta')\left(\frac{\partial U_1}{\partial x}\right)^3 + c_6\left(\frac{\partial U_1}{\partial x}\right)^5\right. \\ & \qquad \left. + (c_7 - c_8\Theta')b^2\left(\frac{\partial V_1}{\partial x}\right)^2\frac{\partial U_1}{\partial x} + c_9 b^4\left(\frac{\partial V_1}{\partial x}\right)^4\frac{\partial U_1}{\partial x} - c_{10}b^2\left(\frac{\partial V_1}{\partial x}\right)^2\left(\frac{\partial U_1}{\partial x}\right)^3\right] \\ & + \mathcal{O}\left(E^8 + \partial_x^4 + \vartheta^4\right), \end{aligned} \tag{4.21}$$

with numerical values of coefficients as follows: $c_1 = 1.91\times10^6$, $\gamma_1 = 5.15\times10^5$, $c_2 = 592$, $c_3 = 0.00931$, $c_4 = 2.75\times10^9$, $c_5 = 8.42\times10^6$, $c_6 = 4.56\times10^{11}$, $c_7 = 1811$, $c_8 = 5.64$, $c_9 = 0.728$, $c_{10} = 2.51\times10^3$. The first line in the right-hand side of (4.21) describes linear dispersive elastic waves along the slab, whereas the second line gives the temperature dependent quintic stress-strain relation of the shape memory alloy. Since $\partial V_1/\partial x = \partial^2 U_1/\partial x\partial t$, the remaining lines show effects upon this stress-strain relation due to rates of change of the strain.

Note that to this order of truncation there is no coupling to the bending modes of the slab which to the same error is simply the beam equation

$$\rho\frac{\partial V_2}{\partial t} = -\gamma_2 b^2\frac{\partial^4 U_2}{\partial x^4} + \mathcal{O}\left(E^8 + \partial_x^4 + \vartheta^4\right), \tag{4.22}$$

where $\gamma_2 = 6.36\times10^5$. However, there exists nonlinear coupling between the modes at higher order.

The corresponding energy equation for the temperature is

$$\begin{aligned} C_v\frac{\partial\Theta'}{\partial t} =\ & \kappa\frac{\partial^2\Theta'}{\partial x^2} + (c_{11} + c_{12}\Theta' - c_{13}\Theta'^2)\frac{\partial U_1}{\partial x}\frac{\partial V_1}{\partial x} \\ & + (c_{14} + c_{15}\Theta')\frac{\partial V_1}{\partial x}\left(\frac{\partial U_1}{\partial x}\right)^3 - (c_{16} + c_{17}\Theta')b^2\left(\frac{\partial V_1}{\partial x}\right)^3\frac{\partial U_1}{\partial x} \\ & + c_{18}\frac{\partial V_1}{\partial x}\left(\frac{\partial U_1}{\partial x}\right)^5 - c_{19}b^2\left(\frac{\partial V_1}{\partial x}\right)^3\left(\frac{\partial U_1}{\partial x}\right)^3 - c_{20}b^4\left(\frac{\partial V_1}{\partial x}\right)^5\frac{\partial U_1}{\partial x} \\ & + c_{21}b^2\frac{\partial^2 U_1}{\partial x^2}\frac{\partial^2 V_1}{\partial x^2} + c_{22}b^2\frac{\partial^2 U_2}{\partial x^2}\frac{\partial^2 V_2}{\partial x^2} + \frac{\partial^2}{\partial x^2}\left[-c_{23}b^2\frac{\partial U_1}{\partial x}\frac{\partial V_1}{\partial x}\right] \\ & + \mathcal{O}\left(E^8 + \partial_x^4 + \vartheta^4\right), \end{aligned} \tag{4.23}$$

where $c_{11} = 1.78\times10^5$, $c_{12} = 586$, $c_{13} = 5.94$, $c_{14} = 2.53\times10^9$, $c_{15} = 8.11\times10^6$, $c_{16} = 36.8$, $c_{17} = 0.00761$, $c_{18} = 1.08\times10^{12}$, $c_{19} = 1.016\times10^6$, $c_{20} = 0.0116$, $c_{21} = 1.05\times10^4$, $c_{22} = 5.92\times10^4$, $c_{23} = 5.228\times10^3$. The first line in (4.23) describes the diffusion of heat generated or absorbed by mechanical strains, $\Theta(\partial U_1)/(\partial x)(\partial V_1)(\partial x)$. However, in the thin slab the internal pattern of strains causes a much more complicated distribution of heating and cooling as summarised by the remaining lines. We retain all of these terms in order to be consistent with the quintic stress-strain of the longitudinal

wave equation. Numerical results validating this model can be found in [18]. By using the methodology based upon the centre manifold technique, the mathematical model derived in this section is easily amenable to account for further details of nonlinear dynamics. This methodology provides us with a powerful and *systematic* tool for deriving new efficient mathematical models, and allows us to construct relatively simple, robust and flexible computer codes [**?**, 18].

The algorithm presented here is based on the construction of the linear approximation as an initial iteration for the algorithm. Then, we achieve the required accuracy in an iterative manner, as described in [28] by computing the residual, computing corrections to the centre manifold, and updating the approximations. The computation of the residual are via a direct coding of the governing equations. This means that if we want to improve the original model (e.g. by using improved constitutive equations, by introducing new internal state variables, and/or incorporating new effects such as porosity, plasticity [27], by using the finite strain framework, different uniaxial and multiaxial conditions [24], different forms of the free energy function [10, 22], etc.) we can do that in a straightforward manner by using the proposed algorithm.

5 Concluding remarks

Models describing SMA are based on strongly coupled system of nonlinear partial differential equations, allowing many modes of behaviour some of which are often little practical importance for engineering applications. Such models can be considered as infinite-dimensional dynamic systems in a way described in Section 4. Based on this idea, we have presented a systematic approach to modelling of nonlinear dynamics of shape-memory-alloy materials using a computer algebra technique and effective differential-algebraic integrators. Two mathematical models have been considered. The first model, based on the Landau-Devonshire representation of the free energy function, provides a good approximation to the shape-memory-alloy dynamics in the case when the bar can be modelled by a thin rod with a shape memory alloy core. As an alternative, we propose a novel model which has been derived directly from the three-dimensional model for shape-memory-alloy evolution, using the centre manifold method. As a basis for the construction of the second model, we have used the Falk-Konopka representation of the free energy function, developed for the three-dimensional case. This representation does not explicitly involve strain-gradient terms. The considered problems are strongly nonlinear and present a computational challenge that require robust numerical procedures. We have developed such procedures using a reduction of the original system of partial differential equations to a system of differential-algebraic equations (DAE). For the solution of this system we have applied a robust DAE integrator and demonstrated its efficiency on the calculation of nonlinear effects describing phase transitions in shape-memory alloys.

We described in detail the main features of our approach based on the fact that the essential dynamics of a higher-dimensional system can be reduced to a lower-dimensional centre manifold. We showed that the essential dynamics of complicated behaviour of the SMA materials can be determined by the evolution of a *subset* of the possible, critical modes, and we demonstrated how low-dimensional models for the evolution of the amplitudes of these modes on such a manifold can be constructed.

Acknowledgements A partial support of the Australian Research Council (Grant 179406) and a travel grant to present a part of this work at a workshop on New Methods in Applied and Computational Mathematics are gratefully acknowledged. We thank Kerryn Thomas for her contributions to the results of computational experiments.

References

[1] F. Auricchio and E. Sacco, A one-dimensional model for superelastic shape-memory alloys with different elastic properties between austenite and martensite, Int. J. Non-Linear Mech. **32**, 1101–1114 (1997).
[2] F. Balta and E. S. Suhubi, Theory of nonlocal generalised thermoelasticity, Int. J. Eng. Sci. **15**, 579–588 (1977).
[3] M. Brokate, Hysteresis operators. In: Phase Transition and Hysteresis, edited by Brokate et al. (Springer-Verlag, 1994), pp. 87–146.
[4] C.-K. Chen and P. C. Fife, Nonlocal models of phase transitions in solids, Preprint (Department of Mathematics, University of Utah, 2000).
[5] S.-N. Chow, W. Liu, and Y. Yi, Center manifolds for invariant sets, J. Diff. Equations, **168**, 355–385 (2000).
[6] F. Falk, Model free energy, mechanics, and thermodynamics of SMA, Acta Metall. **28**, 1773–1780 (1980).
[7] F. Falk and P. Konopka, Three-dimensional Landau theory describing the martensitic phase transformation of SMA, J. Phys.: Condens. Matter **2**, 61–77 (1990).
[8] M. Fremond, Shape memory alloys. A thermomechanical model. In: Free Boundary Problems: Theory and Applications, edited by K.-H. Hoffmann and J. Sprekels (Longman Scientific & Technical, 1990) pp. 295–306.
[9] B. Garcia-Archilla and E. S. Titi, Postprocessing the Galerkin method, SIAM J. Numer. Anal. **37**(2), 470–499 (2000).
[10] J. M. Golden, Consequences of non-uniqueness in the free energy of materials with memory, Int. J. Eng. Sci. **39**, 53–70 (2000).
[11] S. Govindjee and G. J. Hall, A computational model for shape memory alloys, Int. J. Solids Struct. **37**, 735–760 (2000).
[12] K.-H. Hoffmann and M. Niezgodka, Mathematical models of dynamical martensitic transformations in shape memory alloys, J. Intell. Mater. Syst. Struct. **1**, 355–374 (1990).
[13] K.-H. Hoffmann and J. Zou, Finite element approximations of Landau-Ginzburg's equation model for structural phase transitions in shape memory alloys, M^2AN **29**, No. 6, 629–655 (1995).
[14] O. Klein, Stability and uniqueness results for a numerical approximation of the thermomechanical phase transitions in SMA, Advances in Mathematical Sciences and Applications (Tokyo) **5**, No. 1, 91–116 (1995).
[15] P. Krejci and L. Sprekels, Phase-field models with hysteresis, J. Math. Anal. Appl. **252**, 198–219 (2000).

[16] C. R. Laing, A. McRobie, and J. M. T. Thomson, The post-processed Galerkin method applied to nonlinear shell vibrations, Dyn. Stab. Syst. **14**(2) (1999).
[17] C. Lubich, On dynamics and bifurcations of nonlinear evolution equations under numerical discretization. In: Ergodic Theory, Analysis, and Efficient Simulation of Dynamical Systems, edited by B. Fiedler (Springer, Berlin, 2001) pp. 469–500.
[18] R. V. N. Melnik, A. J. Roberts, and K. A. Thomas, Computing dynamics of copper-based SMA via centre manifold reduction of 3D models, Computational Materials Science **18** (3-4), 255–268 (2000).
[19] R. V. N. Melnik, Discrete models of coupled dynamic thermoelasticity for stress-temperature formulations, Appl. Math. Comp. **122**, 107–132 (2001).
[20] R. V. N. Melnik, A. J. Roberts, and K. A. Thomas, Coupled thermomechanical dynamics of phase transitions in shape memory alloys and related hysteresis phenomena, Mech. Res. Commun. **28**(6), 637–651 (2001).
[21] R. V. N. Melnik, A. J. Roberts, and K. A. Thomas, Phase transitions in shape memory alloys with hyperbolic heat conduction and differential-algebraic models, in preparation.
[22] I. Muller and S. Seelecke, Thermodynamic aspects of shape memory alloys, Math. Comp. Model. **34**, 1307–1355 (2001).
[23] M. Niezgodka and J. Sprekels, Convergent numerical approximations of the thermomechanical phase transitions in SMA, Numer. Math. **58**, 759–778 (1991).
[24] E. Patoor, W. Entemeyer, A. Eberhardt, and M. Berveiller, Stress-induced martensitic transformation in polycrystalline alloys, ZAMM **80**, S2, S443–S444 (2000).
[25] V. A. Pliss, Principal reduction in the theory of stability of motion, Izv. Akad. Nauk. SSSR. Mat. Ser. **28**, 1297–1324 (1964).
[26] V. A. Pliss and G. Sell, Approximation dynaamics and the stability of invariant sets, J. Diff. Equations **149**, 1–51 (1998).
[27] M. A. Qidwai and D. C. Lagoudas, On thermomechanics and transformation surfaces of polycrystalline NiTi shape memory alloy material, Int. J. Plasticity **16**, 1309–1343 (2000).
[28] A. J. Roberts, Low-dimensional modelling of dynamics via computer algebra, Comput. Phys. Commun. **100**(3), 215–230 (1997).
[29] A. J. Roberts, Computer algebra derives correct initial conditions for low-dimensional dynamical models, Comput. Phys. Commun. **126**, 187–206 (2000).
[30] A. J. Roberts, Holistic discretization ensures fidelity to Burgers' equation, Appl. Numer. Math. **37**, 371–396 (2001).
[31] J. C. Robinson, Computing inertial manifolds,
Discrete and Continuous Dynamical Systems, to appear.
[32] J. Sijbrand, Properties of center manifolds,
Trans. Amer. Math. Soc. **289**, 31–469 (1985).
[33] J. Sprekels, Shape memory alloys: Mathematical models for a class of first order solid-solid phase transitions in metals, Control Cybern. **19**, 287–308 (1990).
[34] D. V. Strunin, R. V. N. Melnik, and A. J. Roberts, Coupled thermomechanical waves in hyperbolic thermoelasticity, J. Therm. Stresses **24**, 121–140 (2001).